TECHNICAL MEMO

PREPARED BY: DAVID JOHNSON (PURDUE UNIVERSITY), JORDAN FISCHBACH (RAND CORPORATION), NATHAN GELDNER (PURDUE UNIVERSITY), MICHAEL WILSON (RAND CORPORATION), CHUCK STELZNER (RAND CORPORATION)

DATE: FEBRUARY 2021

RE: UPDATED METHODS SUMMARY: COASTAL LOUISIANA RISK ASSESSMENT MODEL FOR 2023 COASTAL MASTER PLAN

THE FOLLOWING TECHNICAL MEMO IS AN INTERIM REPORT TO BE REVISITED AND UPDATED AFTER THE INITIAL RESULTS FROM THE 2023 COASTAL MASTER PLAN'S EXISTING CONDITIONS AND FUTURE WITHOUT ACTION LANDSCAPE MODEL RUNS ARE AVAILABLE.

1.0 INTRODUCTION

The Coastal Louisiana Risk Assessment (CLARA) model was originally created by researchers at RAND Corporation to support development of Louisiana's 2012 Coastal Master Plan. It is designed to estimate flood depth exceedances, direct economic damage exceedances, and expected annual damage from tropical cyclones that that make landfall in or near the Louisiana coastal zone. The model uses high-resolution hydrodynamic simulations of storm surge and waves as inputs. Monte Carlo simulation is used to estimate risk under a range of assumptions about future environmental and economic conditions and with different combinations of structural and nonstructural risk reduction projects on the landscape.

CLARA has been applied to estimate coastal flooding and flood risk reduction for a range of applications since 2012. The model was significantly updated to inform the 2017 Coastal Master Plan (CLARA v2.0; see Fischbach et al., 2017). Subsequently, the model development team completed another series of improvements in 2019-2020 to prepare for the 2023 Coastal Master Plan analysis, leading to the third major version of CLARA. These improvements are documented in detail in a separate report (Fischbach et al., 2021).

This document provides an overview of the CLARA v3.0 methodology and model as applied for the 2023 Coastal Master Plan. Specifically, this memo presents the overall risk framework applied, describes the approach for translating a sample of high-resolution hydrodynamic simulations into statistical estimates of flood depth annual exceedance probabilities (AEPs), and summarizes the methods applied to estimate asset damage and other direct economic impacts. This summary is intended to serve as an overview of the modeling approach as applied for CLARA v3.0 for a technical audience.

2.0 MODEL OVERVIEW

RISK FRAMEWORK

Risk is broadly defined as the possibility of experiencing an injury or loss. While many different quantitative frameworks for risk assessment are used by varied disciplines, the CLARA model defines risk as the product of the value of a loss and the probability of experiencing it from a particular hazardous event. Damage is caused by storm surge-based flooding, and the probability of experiencing a given level of flooding is broken into two components, hazard and vulnerability. **Hazard** is defined as the probability of observing a tropical cyclone with a particular set of characteristics capable of producing flooding in the coastal Louisiana region. **Vulnerability** is the probability of the storm event producing a given level of flooding, determined not only by storm surge and wave dynamics but also by interactions with engineered levees, floodwalls, gates, and pumps. The **consequences** estimated in CLARA are direct economic damage resulting from inundation (wind and surge velocity damage are excluded). This three-part risk framework of hazard, vulnerability, and consequences stems from the risk literature and has been used in other studies of coastal flood risk analysis (Morgan & Henrion, 1990; U.S. Army Corps of Engineers (USACE), 2009a; Fischbach, 2010).

Any tropical cyclone that makes landfall in close enough proximity to coastal Louisiana and Mississippi is included in CLARA's risk calculations. Storms are parameterized using five characteristics at landfall, their central pressure, radius of maximum windspeed, forward velocity, and longitudinal location and heading. Conditional upon a storm event occurring, the relative likelihood of it being a storm with a specific combination of parameters is determined using a joint probability model adapted from previous applications of the joint probability method with optimal sampling (JPM-OS) (Resio, 2007; Interagency Performance Evaluation Taskforce, 2009; Resio et al., 2009; Johnson et al., 2013; Fischbach et al., 2017; Nadal-Caraballo et al., 2020).

The model emphasizes uncertainty quantification through Monte Carlo simulation and techniques for analytic uncertainty propagation. It accounts for uncertainty in storm surge and wave levels, noise in Lidar measurements of topographic elevations, physical variability of overtopping rates, the possibility of levee/floodwall breaches, and randomness in the historical record of observed storms. Losses are calculated as a deterministic function of inundation depths and structural attributes, but the model does consider uncertainty in those attributes for both existing and future structural assets. Losses are limited to direct economic damage. This includes damage to structures, their contents and inventory, but also losses incurred during a restoration period such as lost wages and rents, costs associated with evacuation and temporary displacement, etc. Results are expressed in terms of flood damage at different annual exceedances probabilities, and an overall average across the distribution of plausible storm events (expected annual damage, or EAD).

MODEL STRUCTURE

From the original 2012 development, CLARA has been organized into three basic modules, shown in Figure 1 below (Fischbach et al., 2012). The model uses the **input preprocessing module** to prepare hydrodynamic and geospatial information and estimate statistics for flood depths for areas of the coast without enclosed protected systems. The **flood depth module** uses storm surge and wave inputs to estimate overtopping, structure fragility, and interior drainage within enclosed protected systems, such as the Greater New Orleans Hurricane and Storm Damage Risk Reduction System (HSDRRS). Finally, the **economic module** develops estimates of assets at risk based on a detailed inventory of coastal assets and uses flood depth inputs from the prior modules to estimate damage from events of different severity and recurrence. The direct economic impacts are summarized into damage exceedances and EAD.

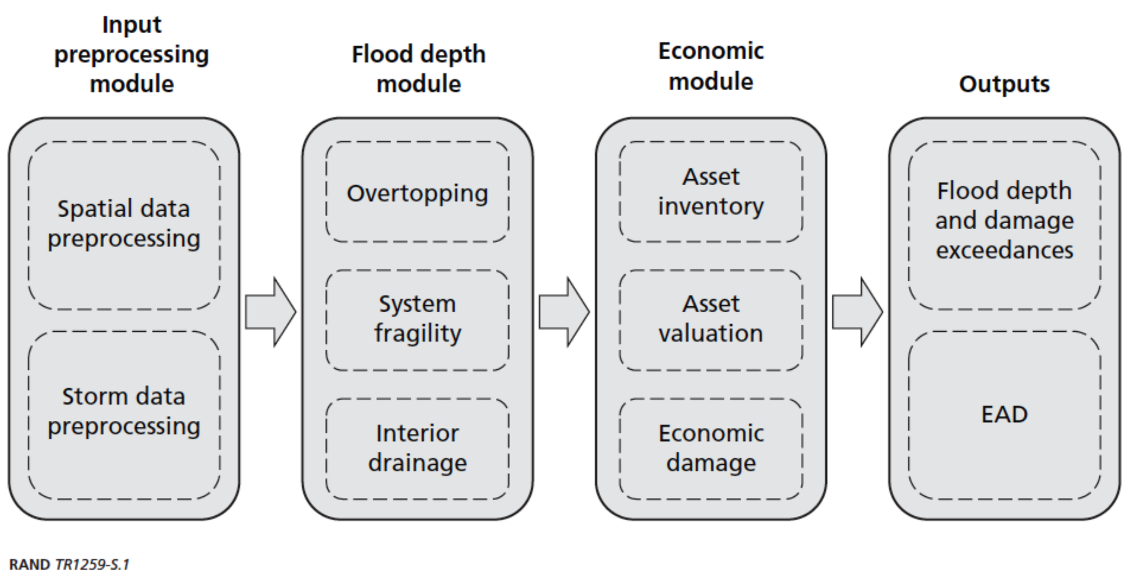

Figure 1. The CLARA model structure (Source: Fischbach et al., 2012).

GEOSPATIAL SCOPE AND UNIT OF ANALYSIS

The CLARA model's spatial domain is shown in Figure 2. It consists of the Louisiana coastal zone, extending inland to encompass the 2,000-year floodplain as projected 50 years into the future, and the entirety of Mississippi's three coastal counties (Hancock, Harrison, and Jackson). This domain is subdivided into a mixed-resolution grid of 126,174 polygons. Each grid polygon is paired with a single grid point which, in areas unenclosed by protection systems, is the location from which storm surge and wave data are extracted from the coupled ADCIRC+SWAN model. Within enclosed protection systems, the grid point is where still-water elevation and flood depth exceedances are calculated.

Figure 2. The CLARA model's spatial domain (Source: Fischbach et al., 2021).

The spatial domain and resolution have been adjusted in each successive version of CLARA, so the shape and location of its current grid polygons and points are derived in part from legacy features. However, the polygons and points are defined to have the following essential features:

1. The boundaries of grid polygons do not cross the boundaries of census blocks, Census-defined municipalities and incorporated places, existing and proposed levee/floodwall centerlines, major bodies of water (e.g., Mississippi and Atchafalaya rivers), and voids in the ADCIRC mesh along weir lines. This implies, for example, that every census block contains at least one grid polygon (which could possibly be the entire block); conversely, no grid polygon contains portions of more than one census block.
2. Grid points are spaced at a resolution no coarser than a regular 1-km grid. Thus, the grid has higher resolution in areas with census blocks smaller than 1 km^2.
3. If a census block is small enough that it would contain no points of a regularly spaced 1-km grid, a grid point corresponding to that block's grid polygon is placed at the polygon centroid (or snapped to the nearest interior point if the centroid falls outside the polygon).
4. If a census block contains more than one point in a regularly spaced 1-km grid, then it is subdivided into multiple polygons defined so that every location interior to a grid point's corresponding polygon is closer to that grid point than any other (i.e., as Thiessen polygons).

The Louisiana and Mississippi coastal zone is very flat, so surge and wave characteristics at each grid point are taken to be representative of the characteristics everywhere within the corresponding grid polygon. When assessing risk to structural assets, however, flood depths are adjusted by the difference in topographic elevations between the locations of each grid point and a particular asset.

3.0 ESTIMATING FLOOD DEPTHS

HAZARD CHARACTERIZATION AND SYNTHETIC STORMS

The model is designed to estimate risk of storm surge-based flooding from any tropical cyclone event impacting the study domain. The conception of hazard is the probability of an event occurring with a specified set of storm characteristics at landfall. To estimate this, the basic JPM-OS approach is adopted (Resio, 2007; Resio et al., 2009; Nadal-Caraballo et al., 2020). Storms are parameterized using five variables: central pressure c_p in millibars (mb), radius of maximum windspeed r in nautical miles (nm), forward velocity v_f in knots (kt), location of landfall x in degrees longitude[1], and landfall heading θ_l in radial degrees east of due north. A joint probability distribution function (PDF) is then fit by applying maximum likelihood to the historical record of observed cyclonic events.

CLARA modifies the joint PDF described in Resio (2007) by using a lognormal distribution for r_{max} rather than a normal distribution. A linear drift term is incorporated for the location parameter of the central pressure's Gumbel distribution, which allows the average central pressure of tropical cyclones to vary over time. The resulting joint PDF is as follows:

$$\Lambda(c_p, r, v_f, \theta_l, x) = \Lambda_1 \cdot \Lambda_2 \cdot \Lambda_3 \cdot \Lambda_4 \cdot \Lambda_5$$

$$\Lambda_1 = f(c_p|x) = \frac{\partial}{\partial x}\left\{\exp\left\{-\exp\left[-\frac{c_p - (a_0(x) + a_1(x)t)}{a_2(x)}\right]\right\}\right\}$$

$$\Lambda_2 = f(r|c_p) = \frac{1}{r\sigma(\mathrm{c_p})\sqrt{2\pi}} e^{-\frac{\left(\ln r - \bar{r}(c_p)\right)^2}{2\sigma^2(c_p)}}$$

$$\Lambda_3 = f(v_f|\theta_l) = \frac{1}{\sigma\sqrt{2\pi}} e^{-\frac{\left(\overline{v_f}(\theta_l) - v_f\right)^2}{2\sigma^2}}$$

$$\Lambda_4 = f(\theta_l|x) = \frac{1}{\sigma(x)\sqrt{2\pi}} e^{-\frac{\left(\overline{\theta_l}(x) - \theta_l\right)^2}{2\sigma^2(x)}}$$

$$\Lambda_5 = f(x) = \Phi(x)$$

The historic tropical cyclone parameters at landfall are taken from HURDAT2 data (Landsea & Franklin, 2013), augmented to impute missing values for c_p and r_{max}, as described in Nadal-Caraballo et al. (2020).

The understanding of the relationship between these storm parameters and the resulting storm surge and wave characteristics is based on high-resolution hydrodynamic simulations of a suite of idealized cyclonic events referred to as "synthetic storms". Simulations are not restricted to historic events;

---

[1] CLARA utilizes an idealized Louisiana coastline represented by a straight line west to east at $29.5°N$, implying that landfall can be characterized only by the longitudinal location.

using synthetic storms allows for the sampling of the parameter space in a balanced way. To estimate the flood depth AEP distribution, both the flood depths produced by each synthetic storm, and the relative likelihood of observing a real storm with parameters more similar to a given synthetic storm than any other need to be known.

The process of selecting which synthetic storms to run through a coupled ADCIRC+SWAN model is an analytic challenge unto itself; Fischbach et al. (2021) describes how this was done to support Louisiana's 2023 Coastal Master Plan, and other literature for background on this problem (Irish et al., 2009; Fischbach et al., 2016; Zhang et al., 2018). Once a synthetic storm suite S has been selected, the space of storm parameters is partitioned into rectangular cells defined by restricting each parameter to a continuous interval. The bounds of the intervals for each cell are set so that a single synthetic storm occupies each cell, with endpoints equidistant between the parameter values of the synthetic storm and those in adjacent cells. The hazard associated with each synthetic storm is thus calculated as the probability mass found by integrating the estimated joint PDF over the bounds of a synthetic storm's cell of the parameter space.

FLOOD DEPTHS IN UNENCLOSED AREAS

Individual synthetic storms are assumed to produce a still-water flood elevation in areas not enclosed by a ringed protection system equal to the peak surge elevation from the surge hydrograph. The peak flood depths associated with a synthetic storm are thus calculated as the sum of the peak surge elevation and the free wave crest height, (i.e., the average height of waves above mean surge elevations) minus the topographic elevation. The coupled ADCIRC+SWAN model reports the significant wave height, which is first restricted to a value no greater than 0.78 times the still-water flood depth to account for the physics of wave breaking. The depth-limited significant wave height is then converted to a free wave crest height by multiplying it by 0.7 (Federal Emergency Management Agency (FEMA), 2020).

FLOOD DEPTHS WITHIN ENCLOSED PROTECTION SYSTEMS

In areas enclosed by a ring of protection features (e.g., levees, floodwalls, gates), storm surge and waves interact with the protection features, possibly leading to water entering the protected polder(s) through overtopping and/or breaches caused by system failure. On the system interior, peak still-water flood elevations are governed not by the surge and wave dynamics themselves, but by the net volume of water in the system (i.e., overtopping and breach volumes, plus rainfall, minus any water pumped back out) and how that water routes between interior polders through interior drainage.

CALCULATING SURGE AND WAVE OVERTOPPING

Depending on the elevation of storm surge relative to the crown elevation of a protection system, CLARA applies different equations to calculate the rate of overtopping from surge and/or wave action. Overtopping dynamics also vary in the presence of a floodwall, or floodwall on top of a levee, compared to a levee alone. If storm surge is below the crown of a protection feature, water may enter the system interior via waves breaking over the top of the barrier. At times when storm surge rises above the crown, the surge flows freely into the system in addition to the wave overtopping.

CLARA calculates a two-dimensional overtopping rate at each reach point (e.g., cubic feet per second per linear foot of reach segment) and over each time period in the surge hydrograph. It is then converted to an overtopping volume by multiplying the rate by the 15-minute time interval of the hydrograph and the linear length of the reach segment represented by the given reach point. These calculations occur at a series of "reach points" spaced at intervals typically no more than 300 m apart, with points that represent smaller segments placed at sharp bends in an alignment, transitions between levees and floodwalls, gates, or the locations of pumping stations. Volumes are then summed over the three-day duration of the hydrograph to produce the total volume of water entering the system interior over the reach segment corresponding to each reach, which is then aggregated to the polder level.

SURGE OVERTOPPING

During time intervals when storm surge is higher than the crown of protection structures, a free weir equation is used to calculate the rate at which water flows continuously into the system:

$$q = c_w(\eta - z_c)^{3/2}$$

Here, q is the flow rate in cubic meters per second, η is the surge elevation (m), z_c the crown elevation (m), and c_w a weir coefficient based on the geometry of the flood barrier that captures the extent to which the geometry affects the flow over the weir. CLARA uses values taken from a prior study of the HSDRRS system: $1.68 \ \ m^{1/2}/s$ for floodwalls, $1.45 \ \ m^{1/2}/s$ for levees, and $1.12 \ \ m^{1/2}/s$ for flood gates (Interagency Performance Evaluation Taskforce, 2009).

Overtopping associated with the waves situated atop storm surge is handled separately from the weir flow equation, as described below.

WAVE OVERTOPPING

Wave data are extracted from the coupled ADCIRC+SWAN model as the significant wave height (H_{200}) at points approximately 200 m in front of the protection feature base, so a wave breaking equation is first applied to calculate the depth-limited significant wave height at the toe of the structure, H_s:

$$H_s = \min(H_{200}, \gamma(\eta - z_{base}))$$

The value of the wave-breaking parameter η is assumed to be 0.4 for standard levee and floodwall geometries, and z_{base} represents the topographic elevation at the toe of the structure base. CLARA by default assumes that $z_{base} = 0$ for protection features located in the flat plain of Louisiana's coastal zone.

Given the spectral wave period T, the surf similarity parameter ξ_0 is then calculated, which conveys how much of the kinetic energy of the waves is dissipated through breaking and how much is applied to conveying the waves over the barrier. Where $\tan\alpha$ is the frontside slope of the levee feature (assumed to be 0.25) and $g = 9.81 \ m/s^2$ is the standard acceleration under gravity,

$$\xi_0 = \tan\alpha \cdot \sqrt{\frac{gT^2}{2\pi H_s}}$$

According to van der Meer (2002), different formulas should be used to calculate overtopping rates in different regimes for ξ_0. If $\xi_0 \leq 5$ and the surge elevation is below the crown elevation of a levee (such that $z_c - \eta > 0$), then the rate is

$$q = \frac{0.47\sqrt{gH_s^3}}{\sqrt{\tan\alpha}}\xi_0 \exp\left(-3.325\frac{z_c - \eta}{H_s\xi_0\gamma_v}\right)$$

where γ_v is a geometry influence parameter set to 0.65 if a floodwall is placed on top of the levee and 1 otherwise. By default, CLARA treats overtopping rates as stochastic with variability consistent with previous USACE studies (USACE, 2009a). The coefficient -3.325 above is the mean value of a normally distributed random variable with standard deviation equal to 0.495.

In the case of $\xi \geq 7$,

$$q = 10^{-0.92}\sqrt{gH_s^3}\exp\left(-\frac{R_c}{H_s(0.33 + 0.022\xi_0)}\right)$$

When simulating variability in overtopping in this regime, -0.92 is the mean value of a normally distributed random variable with a standard deviation of 0.24. Between these two regimes (i.e., $5 < \xi_0 < 7$), the rate is determined by linear interpolation on the values of $\log q$ for $\xi_0 = 5$ and $\xi_0 = 7$.

When waves encounter a floodwall that is freestanding, rather than sitting atop a levee, the rate is calculated using a formula from Franco and Franco (1999):

$$q = 0.082\sqrt{gH_s^3}\exp\left(-\frac{3.614R_c}{H_s}\right)$$

Lastly, in the case where surge is above the crown of a protection feature, surge overtopping is expressed as $q = 0.13\sqrt{gH_s^3}$. As such, the combined surge and wave overtopping is calculated as:

$$q = C_w(\eta - z_c)^{3/2} + 0.13\sqrt{gH_s^3}$$

ESTIMATING THE PROBABILITY AND CONSEQUENCES OF SYSTEM FAILURES

In order to properly estimate the probability of flooding, the probability and consequences of protection system failure must also be considered. A protection system failure is defined here as an event in which the system suffers structural damage, allowing water to enter the polder at an elevation below the crown elevation of the protection system.

CLARA models the probability of system failure as a function of the combined surge and wave overtopping rate for two distinct failure modes. The first is **overtopping failure**, wherein overtopped water erodes the back side of a protection feature, reducing its ability to withstand loading on the front side to the point where structural integrity is lost. The second is **seepage failure**, which occurs when water is pressed through the soil at the base of the protection feature, exerting upward pressure that causes internal erosion leading to rotation or cracking that causes catastrophic breaching. Previous versions of CLARA also considered slope stability failures, but analysis of initial results from the 2017 Coastal Master Plan found the probability of this failure mode to be sufficiently smaller than the others to justify eliminating it to improve computational efficiency.

Previous studies of protection systems in coastal Louisiana assumed a step function for the probability of failure from backside scour (i.e., erosion) as a function of overtopping rates or the differential between surge elevation and the crown of protection elements. CLARA v3.0 instead assumes that the probability of a breach can be represented by a continuous, sigmoidal curve of the form:

$$P_L(x) = \frac{p_{max}}{1 + e^{-k(x-x_c)}}$$

where $P_L(x)$ is the probability of failure for a reach of characteristic length L meters, x the overtopping rate in cubic meters per second per linear meter of levee/floodwall, p_{max} the maximum probability of failure, k a parameter characterizing the sensitivity of breach probability to changes in x, and x_c a critical overtopping rate at which the probability of failure reaches half its maximum value. The failure probability for a reach of length l meters is then calculated under an assumption that failures are independent between reach segments, as:

$$P(x, l) = 1 - \left(1 - P_L(x)\right)^{l/L}$$

Gates and other transition features are assumed to have the same two-dimensional probability of failure as the nearest adjacent levee or floodwall on either side.

There is limited empirical evidence to estimate the true underlying probability distribution $P(x)$. CLARA thus allows for any set of L, p_{max}, k, and x_c parameters to be used. To be consistent with the previously-mentioned studies by USACE, though, the analysis typically uses curves that have been parameterized so that they pass through the points on the step functions assumed by those efforts (Interagency Performance Evaluation Taskforce, 2009; USACE et al., 2013). The model can also operate in an overtopping-only mode that assumes protections systems do not fail under any load.

For each synthetic storm, CLARA runs a number of Monte Carlo replicates of overtopping and system failure across each reach point along the centerlines of enclosed protection systems. For each replicate, a uniform random variate is drawn from $[0,1]$ for each reach segment. The probability of failure is calculated at each time interval of the hydrograph, and failure occurs at the earliest time period where the probability equals or exceeds the random variate's value.

Whenever a failure is projected to occur, it is assumed that the breach is full-depth and full-length, effectively reducing the crown elevation of the protection elements to the base elevation for the entire length of the reach segment that fails. Note that because reaches in CLARA are divided into segments that are nearly always 300 m or less in length, the full-length breach assumption is not as catastrophic as other studies which often assume reaches that may be miles long. From the time period when a failure occurs onward, the same free weir equation from the overtopping module is used to calculate the volume of water entering the system through the failed segment with the crown elevation reduced to the base elevation.

INTERIOR DRAINAGE

CLARA uses a simplified, gravity-based model of interior drainage to translate volumes of water inside a protection system to a peak still-water elevation at any interior point. The interiors of enclosed protection systems are divided into polders — regions that are hydrologically independent of each other up to a certain elevation — which are often demarcated by a natural ridge, roadway, or other elevated feature. The spatial definitions of polders in CLARA were taken from USACE's post-Katrina Louisiana Coastal Protection and Restoration (LACPR) study (USACE, 2009a).

Thus, water that enters a polder (through overtopping, breaches, or rainfall) initially remains in that region, filling it until the still-water elevation reaches a level wherein water begins to spill over into an adjoining polder. That level is referred to as an **interflow elevation**; between any two adjacent polders, the interflow elevation is defined as the lowest topographic elevation along their shared border. The relationship between the volume of water in a polder and the still-water elevation it produces is called a **stage-storage curve** and is calculated by GIS analysis of the polder's digital elevation model (DEM). It is effectively the volume of open air, V, below a given elevation, E. For a polder P,

$$V(E) = \sum_{p \in P} A_p \cdot \max[E - e_p]$$

where p is any pixel of the DEM in P, A_p is the area of the pixel (e.g., $A_p = 900 \ \ m^2$ for a DEM with 30-meter resolution), and e_p is the topographic elevation of the pixel (or initial water surface elevation if the pixel is open water). The initial volume of water in a polder is calculated as the sum of overtopping, breach, and rainfall volumes, minus pumping volumes (over all time periods). The inverse of the above relationship is used to translate the water volume to an initial still-water elevation. It is assumed that pumping stations operate continuously over the time of nonzero surge at points exterior to a protection system. Because pumps are designed primarily to prevent flooding from rainfall events, it is assumed that they operate at 50% of their rated capacity to account for the likelihood of some pumps being overwhelmed or offline for maintenance. While this may not reflect actual operations, sensitivity analysis for the 2012 Coastal Master Plan indicated that this assumption does not have a substantial effect on interior flood exceedances (Fischbach et al., 2012).

The interior drainage algorithm then distributes water between adjacent polders until reaching an equilibrium characterized by one of the following conditions for all pairs of adjoining polders: (1) water elevations in adjoining polders are equal; (2) if not equal, the water elevations are less than or equal to the interflow elevation between the polders. If two adjacent polders are not in equilibrium, it implies that the water elevations are unequal and that at least one level is above the interflow elevation, meaning that water would flow from the higher polder to the lower until equilibrium is reached. Full details of the algorithm used to achieve equilibrium are provided in Johnson et al. (2013).

Some large protection systems such as HSDRRS have secondary levees or floodwalls on the interior as an additional layer of protection against inundation. In these areas, the interior drainage algorithm runs once to distribute the initial water volumes, taking into account the crown height of the secondary protection features when determining the interflow elevation between polders. The differential still-water elevations on each side of the interior feature are then used to estimate the probability of the element failing. Any failures are treated as full-depth breaches, wherein the interflow elevation is reduced to the base of the feature and the drainage algorithm is re-initialized.

CONSTRUCTING AEP DISTRIBUTIONS

Once the Monte Carlo simulation is complete for all synthetic storms in a given case (i.e., combination of time period and scenario assumptions), the frequency distributions of peak still-water elevation and wave heights are aggregated to estimate the AEP distributions for each quantity. The first step in this process is to construct an empirical cumulative distribution function (CDF) for each metric at each location describing the probability of experiencing a given level of flooding, conditioned on the occurrence of some storm event. This conditional CDF is then combined with an estimated storm recurrence rate to produce an AEP distribution describing the probability of a level of flooding occurring or being exceeded in a given year.

CALCULATING CONDITIONAL EXCEEDANCE PROBABILITIES

For the purpose of this description, the goal is to produce still-water elevation exceedances; the same procedure can be used for wave height or flood depth exceedances. To generate the event-conditional CDF for a given Monte Carlo replicate, the unique still-water elevations, E, are rank-ordered over all synthetic storms, then weight each value by the probability masses associated with the storm that produced it. The CDF is thus

$$F(e) \coloneqq P(E \leq e) = \sum_{s \in S} \sum_{E \leq e} P(s)$$

where e is the still-water elevation value of interest, and $P(s)$ is the probability mass associated with synthetic storm s in the simulated storm suite S (see Section 0).

CALCULATING ANNUAL EXCEEDANCE PROBABILITIES

The arrival of tropical cyclones is modeled as a Poisson process with a mean arrival rate of α storms per hurricane season. The value of α is estimated using the historical HURDAT2 data to count the number of storms making landfall within three degrees longitude of the study domain since 1950. This allows for the possibility of experiencing more than one storm per year, with the probability of observing κ storms in a year given by

$$P(\kappa) = \frac{e^{-\alpha} \alpha^{\kappa}}{\kappa!}$$

The y-year flood depth exceedance, d_y, is defined as the depth with a probability $1/y$ of occurring or being exceeded in a given year. This implies that the maximum flood depth in a given year has a probability $1-1/y$ of being less than or equal to d_y. Where F_{annual} is the CDF for the maximum annual flood depths and F_{storm} is the CDF for a single storm event, the law of total probability implies that

$$F_{annual}(d_y) = \sum_{\kappa=0}^{\infty} F_{storm}(d_y)^{\kappa} \cdot P(\kappa) = e^{-\alpha} \sum_{\kappa=0}^{\infty} \frac{F(d_y)^{\kappa} \cdot \alpha^{\kappa}}{\kappa!}$$

The AEP distribution is calculated over every synthetic storm for the *n*th replicate of each. The Monte Carlo simulation of overtopping and system fragility is initialized with the same random seed for every synthetic storm. When calculating the exceedance curve, the historical record is also bootstrapped. This is done to account for uncertainty in the joint probability distribution of storm parameters associated with the random sample of observed historic storms. It allows for generation of confidence intervals on the AEP distribution.

Because the historical record is short relative to the number of degrees of freedom in the estimated joint probability distribution, each bootstrap is oversampled so that each sample contains four times the number of observations as the historical record. An annual CDF is generated as described above for each bootstrap sample; the procedure of Chung and Lee (2001) is then modified to produce an unbiased estimate of the variance in exceedance values. As detailed in Fischbach et al. (2017):

> *Denote the y-year exceedance estimated using Monte Carlo replicate i and bootstrap sample j as $\hat{\theta}_{i,j}^{y}$. Assume that the historical record contains n storms and that each bootstrap sample contains m storms (as noted above, $m = 4n$ for the current version of CLARA). Denote the exceedance associated with Monte Carlo replicate i and the historical record of storms as $\theta_{h,i}^{y}$. Let the β-quantile value of $\hat{\theta}_{i,j}^{y}$ over all bootstrap samples be $\hat{\mu}_{\beta,i}$.*
>
> *By Chung and Lee (2001), a α confidence interval adjusted for oversampling is*
>
> $$\left[\hat{\theta}_{h,i}^{y} + \sqrt{\frac{m}{n}}\left(\hat{\mu}_{\frac{1-\alpha}{2},i} - \hat{\theta}_{h,i}^{y}\right), \hat{\theta}_{h,i}^{y} + \sqrt{\frac{m}{n}}\left(\hat{\mu}_{\frac{1-\alpha}{2},i} - \hat{\theta}_{h,i}^{y}\right)\right]$$
>
> *Therefore, an order-preserving transformation of $\hat{\theta}_{ij}^{y}$ is made for every Monte Carlo replicate and bootstrap sample:*
>
> $$\gamma_{i,j}^{y} = \hat{\theta}_{h,i}^{y} + \sqrt{m/n}\,(\hat{\theta}_{i,j}^{y} - \hat{\theta}_{h,i}^{y})$$
>
> *With this adjusted test statistic, the empirical $(1-\alpha)/2$ and $(1+\alpha)/2$ quantile values of $\gamma_{i,j}^{y}$ can now be used to form confidence bounds for θ^{y}.*

4.0 ESTIMATING FLOOD CONSEQUENCES

Estimating flood depth exceedances alone is insufficient for planning purposes, as such information cannot be easily aggregated over space and time. Policy makers are unlikely to invest in flood risk reduction without an understanding of the expected reduction in economic losses the projects would achieve. CLARA therefore estimates the direct economic damage associated with given levels of flooding, producing both annual exceedance probabilities for damage and aggregated EAD. Damage in future time periods can be discounted to generate a present value, allowing us to convert estimates of EAD as it changes over time to a present value of expected losses over a multi-year planning horizon. Expected risk reduction benefits of protection projects can be similarly calculated by comparing expected net present value of damages with and without projects in place.

CLARA largely follows the approach of the Hazus-MH model and post-Katrina LACPR study (FEMA, 2020; USACE, 2009b). Damage estimates include direct economic losses not only to physical assets (e.g., structures, contents, inventories) but also costs borne during repair and reconstruction (e.g., lost wages and rents, temporary displacement/relocation costs). The model does not calculate regional spillover effects (e.g., gasoline price impacts of disruptions to refining capacity, economic output reduction).

The following sections describe (i) the baseline inventory of economic assets in the model domain and their attributes, (ii) how asset inventories and attributes are projected in future scenarios, (iii) valuation of assets, (iv) calculation of losses as a function of flood depths, and (v) construction and aggregation of damage metrics.

ASSET INVENTORY AND ATTRIBUTES

The model's baseline structure inventory is a database of economic assets assembled from multiple sources of structure- and parcel-level data: building footprint polygons developed by Microsoft Corporation (2018); building attributes (e.g., foundation type, foundation height) extracted from Google Street View imagery as described in Chen et al. (under review); the National Structure Inventory v2 (NSI), developed by USACE (Georgist, 2019); ATTOM Data Solutions; and Open Street Maps. Not all data sources contained all structural attributes needed for damage estimation, and some sources had lower quality, estimated, or missing data in certain areas. The full process of matching, prioritizing, and deconflicting these data sources is detailed in Fischbach et al. (2021). The attributes contained in the final merged inventory used by the CLARA damage model are the following:

1. Location (latitude/longitude)
2. Topographic elevation (NAVD88 m) (extracted from digital elevation model at location)
3. Foundation type (e.g., pier, concrete slab)
4. Foundation height / first-floor elevation (m)
5. Square footage of building footprint
6. Total square footage
7. Number of stories
8. Building occupancy type, property use, or business code (e.g., single-family residence)

9. Presence of garage (residential only)
10. Year built

The baseline structure inventory consists of 811,871 buildings in the Louisiana portion of the model domain. Codes representing a building's occupancy, use, or business type are used to select an appropriate function relating the depth of flooding to the resulting level of damage, as well as to determine key parameters related to the asset's replacement cost. Details for both of these uses are given in later sections.

Other assets included in CLARA are vehicles, roads, and agricultural crops. Privately owned vehicle counts are based on 2010 U.S. Census data for the average number of privately owned vehicles per household, and commercial vehicle counts are estimated using Louisiana Department of Motor Vehicles commercial licenses in 2006, adjusted for population change (USACE, 2009b). Roads are calculated as the total lane-miles within each grid polygon as derived from OpenStreetMap. Crop data is sourced from the LSU AgCenter.

MODELING FUTURE POPULATION AND ASSET CHANGE

Future population and economic growth in coastal Louisiana are highly uncertain due to the unknown impacts of future storm events, people's response to slow-moving climate risks, and a transition away from fossil fuels that are a major industrial sector in the region. Studies indicate that the master plan collectively passes a benefit-cost test over a wide range of future states of the world (Fischbach et al., 2019); potential investments in flood protection are thus instead compared to each other on the basis of cost-effectiveness within scenarios. Analyses supporting previous master plans have shown that differences in assumptions about growth do not substantially change the relative ordering of project performance, so the 2023 Coastal Master Plan analysis uses a single population change scenario based on the methods described in Hauer (in preparation). The population is stratified into various demographic groups, and a growth rate is estimated for each at the block group level based on historical census data. Growth is then projected for each group and aggregated to estimate total population changes over time in each block group.

It is assumed that most economic assets (all but roads, crops, and agricultural structures) scale in direct proportion with population change. The number of assets of each type within a grid polygon are changed in future scenarios by the same percentage as the population change within the polygon's parent block group. Fractional numbers of assets are allowed to exist in future inventories.

Once the future number of each asset type has been calculated, new assets are randomly assigned their other attributes by sampling [with replacement] the attributes of other assets of that type in the same grid polygon. This effectively assumes that new assets will have similar characteristics to nearby structures, while accounting for uncertainty in those attributes. In grid polygons experiencing negative growth, the baseline assets to be eliminated from the inventory are randomly selected.

ASSET VALUATION

The model calculates direct economic losses under an assumption that damaged assets are repaired or reconstructed to be made whole again. The relevant valuation as a basis for estimating risk is an asset's replacement cost.[2] The approach to estimating replacement costs is based on the Hazus-MH model, which generally stratifies assets into a set of General Building Stock (GBS) codes according to their use type. Structural assets in CLARA correspond to 33 distinct GBS codes: 11 classes of residential structures, 10 types of commercial buildings, 6 industrial, 2 public sector, 2 educational, and single categories for religious and agricultural structures.

The GBS classification determines what damage categories apply to an asset. For example, agricultural, and some commercial and industrial classes, are assumed to contain inventory stocked for sale which can be damaged, while other classes do not. The replacement cost of a structure (and inventory where applicable) is based on the product of the asset's square footage and an average replacement cost per square foot for that GBS category. Replacement costs for non-inventory building contents (e.g., furnishings, appliances, capital equipment) are valued by multiplying the structural replacement cost by a proportion known as a contents-to-structure value ratio (CSVR). All of the unit costs and CSVR values are taken from the Hazus-MH model (FEMA, 2020), with historical values inflated to 2020 U.S. dollars using an all-sectors consumer price index from U.S. Bureau of Labor Statistics.

Valuation of single-family residences is more complex, with variations in the unit replacement cost per square foot for one- and two-story buildings. The unit cost also varies by construction class, which is a measure of the quality of materials and decorative elements in the structure. Construction class is defined as Economy, Average, Custom, or Luxury, and the proportion of homes in a census block of each class is estimated as a function of the median household income in that block. Additional value is assigned if the residence has an attached garage.

Repair costs for roads, replacement costs for vehicles, and other miscellaneous damage categories (e.g., debris removal and cleanup, landscaping repair) are estimates from the LACPR study (USACE, 2009b).

CALCULATING DIRECT ECONOMIC LOSSES

In the event of a flood, the losses associated with a structural asset are expressed as a proportion of the asset's replacement cost. This proportion is a function of the peak flood depth experienced at the structure's location, measured relative to the first-floor elevation (i.e., depths are reduced by the building's foundation height). This relationship is known as a depth-damage curve. Various curves are

[2] Estimating damage as a proportion of replacement cost is CLARA's default approach. The model can, however, use depreciated value in cases where the age of an asset is known or can be inferred as an option to better approximate reimbursable losses on flood insurance policies using a basis of actual cash value.

reported by FEMA in the Hazus-MH model. The curves used by CLARA vary by occupancy/use type and foundation type. They are estimated from actual insurance claims in Orleans and Jefferson parishes. Different curves exist for damage to the structure, its contents, and inventory. Single-family residences also use distinct curves between 1- and 2-story dwellings. CLARA only accounts for damage resulting from inundation (i.e., not from wind or surge velocity), and its depth-damage curves assume long-duration (greater than 24 hours) inundation from salt water.

The flood depths CLARA uses to calculate damage correspond to 22 AEP values ranging from the 5-year to 2000-year event. n-year depth exceedances d_n are site-specific for structural assets, constructed by summing the surge elevation and wave height exceedances, s_n and w_n, reported at the grid point level, then subtracting the topographic elevation at the location of the asset, e, and the asset's foundation height h:

$$d_n = s_n + w_n - (e + h)$$

In areas enclosed by a protection system, the still-water elevation is considered to be s_n and set $w_n = 0$. Inundation depths for vehicles, roads and crops are calculated using the topographic elevation at the grid point (and setting $h = 0$).

Some damage categories are a function of the time required to repair or demolish and reconstruct assets. Hazus-MH provides estimates for this time as a function of the structural damage. Any building receiving damage greater than half its replacement cost is assumed to be demolished and rebuilt, with lesser degrees of damage incurring shorter restoration periods. The total loss associated with the disruption is calculated by multiplying the duration of the period by the sum of average daily unit costs for lost proprietor's sales, income and wages per square foot; lost rents per square foot; and disruption costs.

DAMAGE METRICS

Once a flood depth and an asset's attributes are estimated, damage is calculated deterministically. Replacement costs are calculated with certainty, and the depth-damage relationships are deterministic; see Section 5.3.3 of Fischbach et al. (2017) for analysis supporting the latter decision. If all relevant information is treated as known, for example, the median estimate of the 1% AEP value for damage is simply the damage associated with the median estimate of the 1% AEP value for flood depths. However, flood depths and structural attributes are uncertain, which necessitates a more sophisticated approach to calculate damage exceedances – particularly when aggregating spatially over multiple assets in the same community.

DAMAGE ANNUAL EXCEEDANCE PROBABILITIES

CLARA estimates the 10th, 50th, and 90th percentile values for surge elevation, wave height, and still-water elevation exceedances. It is assumed that these values follow a normal distribution. This implies that flood depth exceedances are normally distributed, truncated at zero. Damage calculations sample from that distribution, and a Monte Carlo simulation of damage is performed, sampling in each replicate flood depths, imputed values for missing structure attributes, and the attributes of future assets. The result is a distribution of estimated damage exceedance values for each of 22 return periods.

When aggregating damage estimates spatially, note that the Monte Carlo framework draws variates for flood elevations at the grid point level, while asset attributes are sampled at the individual asset level. The resulting distribution of aggregated damage therefore implicitly assumes that flood depths are perfectly correlated within grid points but independent between grid points, and asset attributes are independent. This is a natural consequence of the parametric uncertainty framework; further analysis could lead to more informed assumptions, but it is intuitive that the additional variability in damage estimates associated with uncertainty about these covariance structures is modest compared to the other modeled sources of variability.

EXPECTED ANNUAL DAMAGE

Flood depth exceedances are calculated by accounting for the possibility of experiencing multiple storms in the same hurricane season. When considering damage, a simplifying assumption is made that the total damage to an asset from storms in a single year is equal to the maximum damage incurred by any of the storms alone. Given the long time periods required for post-event restoration, this is believed to be a reasonable assumption.

Therefore, to calculate the expected value of damage in a given year (EAD) the probability that, among m storms occurring in a year, the most severe event is a storm of return period n years must be calculated. This is equivalent to the probability that flood depths from all m storms are less than or equal to the n-year flood depth exceedance.

Denote the set of return periods reported by CLARA as N, where n_i is ordered from high frequency to low (e.g., $n_1 = 5,\ n_2 = 10$). Then the desired probability for n_1 is

$$P_{m,1} = F(n_1)^{m/\alpha}$$

where $F(n_1) = 1 - 1/n_1$ is the CDF value for the n_1-year return period and α is the mean interarrival rate of storm events. For subsequent return periods,

$$P_{m,i+1} = F(n_{i+1})^{m/\alpha} - \sum_{j=0}^{i} P_j$$

This yields the probability associated with each calculated damage exceedance in order to calculate EAD. If the n-year damage exceedance is D_n, then

$$EAD = \sum_{m=0}^{\infty} \sum_{i=1}^{|N|} P_{m,i} \cdot D_{n_i}$$

The β percentile value for EAD is estimated as the value resulting from the formula above when using the β percentile estimate for the damage exceedance at each return period.

DAMAGE OVER TIME

When multiple time periods have been run through CLARA, the results can be used to estimate the present value of expected losses over a multi-year time horizon. EAD changes over time with environmental factors and population/asset changes, so for a time horizon of T years and discount rate d,

$$PV(EAD) = \sum_{t=0}^{T-1} \frac{EAD_t}{(1+d)^t}$$

In practice, it is impractical (and unnecessary) to produce computationally costly ADCIRC+SWAN simulations on an annual basis. Johnson et al. (under review) concludes that storm surge and wave characteristics can be reasonably approximated on a storm by storm basis through linear interpolation over short durations, so estimates of synthetic storm characteristics are constructed and run through CLARA at 5-year intervals. Damage at intermediate years is further interpolated linearly to generate a time series of EAD estimates that are piecewise linear over 5-year increments.

5.0 SUMMARY

CLARA is a state-of-the-art model for assessing direct economic risk from storm surge-based flooding in coastal Louisiana. Through over a decade of development, it has evolved to incorporate ever more realistic representations of physical processes and a thorough accounting of the major uncertainties impacting coastal flood risk. The model is used to evaluate the impacts of investments in structural and nonstructural risk mitigation, as well as coastal restoration, as part of Louisiana's Coastal Master Plan development process. Future versions of this manuscript will include more discussion of the 2023 Coastal Master Plan context and initial results from the plan's Existing Conditions and Future Without Action landscapes.

6.0 REFERENCES

Chen, F.-C., Jahanshahi, M., Johnson, D. R., & Delp, E. (under review). *Deep Learning-based Building Attribute Estimation From Google Street View Images For Flood Risk Assessment Using Feature Fusion and Task Relation Encoding*.

Chung, K.-H., & Lee, S. M. (2001). Optimal bootstrap sample size in construction of percentile confidence bounds. *Scandinavian Journal of Statistics*, *28*(1), 225–239.

Federal Emergency Management Agency. (2020). *Multi-Hazard Loss Estimation Methodology, Flood Model: Hazus-MH Technical Manual* (p. 569). https://www.fema.gov/sites/default/files/2020-09/fema_hazus_flood-model_technical-manual_2.1.pdf

Fischbach, J. R. (2010). *Managing New Orleans Flood Risk in an Uncertain Future Using Non-Structural Risk Mitigation*. RAND Corporation.

Fischbach, J. R., Johnson, D. R., & Groves, D. G. (2019). Flood damage reduction benefits and costs in Louisiana's 2017 Coastal Master Plan. *Environmental Research Communications*, *1*(11), 111001.

Fischbach, J. R., Johnson, D. R., & Kuhn, K. (2016). Bias and efficiency tradeoffs in the selection of storm suites used to estimate flood risk. *Journal of Marine Science and Engineering*, *4*(1), 10.

Fischbach, J. R., Johnson, D. R., Kuhn, K., Pollard, M., Stelzner, C., Costello, R., & Cobell, Z. (2017). *Coastal Master Plan Modeling: Attachment C3-25 – Storm Surge and Risk Assessment*. Louisiana Coastal Protection and Restoration Authority.

Fischbach, J. R., Johnson, D. R., Ortiz, D. S., Bryant, B. P., Hoover, M., & Ostwald, J. (2012). *Coastal Louisiana Risk Assessment Model: Technical Description and 2012 Coastal Master Plan Analysis Results*. https://www.rand.org/pubs/technical_reports/TR1259.html

Fischbach, J. R., Johnson, D. R., Wilson, M. T., Geldner, N. B., & Stelzner, C. (2021). *2023 Coastal Master Plan: Risk Assessment*. Louisiana Coastal Protection and Restoration Authority.

Franco, C., & Franco, L. (1999). Overtopping formulas for caisson breakwaters with nonbreaking 3D waves. *Journal of Waterway, Port, Coastal, and Ocean Engineering*, *125*(2), 98–108.

Georgist, H. (2019). *National Structure Inventory*. https://github.com/HydrologicEngineeringCenter/NSI

Interagency Performance Evaluation Taskforce. (2009). *Performance Evaluation of the New Orleans and Southeast Louisiana Hurricane Protection System, Vol. VIII: Engineering and Operational Risk and Reliability Analysis*. U.S. Army Corps of Engineers.

Irish, J. L., Resio, D. T., & Cialone, M. A. (2009). A surge response function approach to coastal hazard assessment. Part 2: Quantification of spatial attributes of response functions. *Natural Hazards*, *51*(1), 183–205.

Johnson, D. R., Fischbach, J. R., & Ortiz, D. S. (2013). Estimating Surge-Based Flood Risk with the Coastal Louisiana Risk Assessment Model. *Journal of Coastal Research*, *67 (10067)*, 109–126. https://doi.org/10.2112/SI_67_8

Johnson, D. R., Wang, J., Geldner, N. B., & Zehr, A. (n.d.). *Rapid, risk-based levee design framework to achieve greater risk reduction at lower cost than standards-based design*.

Landsea, C. W., & Franklin, J. L. (2013). Atlantic hurricane database uncertainty and presentation of a new database format. *Monthly Weather Review*, *141*(10), 3576–3592.

Microsoft Corporation. (2018). *Computer generated building footprints for the United States*. Microsoft Corporation. https://github.com/microsoft/USBuildingFootprints

Morgan, G. M., & Henrion, M. (1990). *Uncertainty: A Guide to Dealing with Uncertainty in Quantitative*

Risk and Policy Analysis. Cambridge University Press.

Nadal-Caraballo, N. C., Campbell, M. O., Gonzalez, V. M., Torres, M. J., Melby, J. A., & Taflanidis, A. A. (2020). Coastal hazards system: A probabilistic coastal hazard analysis framework. *Journal of Coastal Research*, *95*(SI), 1211–1216.

Resio, D. T. (2007). White paper on estimating hurricane inundation probabilities. In *Performance Evaluation of the New Orleans and Southeast Louisiana Hurricane Protection System. Appendix 8: Hazard Analysis: Vol. VIII*. U.S. Army Corps of Engineers.

Resio, D. T., Irish, J., & Cialone, M. (2009). A surge response function approach to coastal hazard assessment–part 1: Basic concepts. *Natural Hazards*, *51*(1), 163–182.

U.S. Army Corps of Engineers. (2009a). *Louisiana Coastal Protection and Restoration Final Technical Report: Hydraulics and Hydrology Appendix* (p. 389). U.S. Army Corps of Engineers.

U.S. Army Corps of Engineers. (2009b). *Louisiana Coastal Protection and Restoration Final Technical Report: Economics Appendix* (p. 271). U.S. Army Corps of Engineers.

U.S. Army Corps of Engineers, Louisiana Coastal Protection and Restoration Authority, & Terrebonne Levee & Conservation District. (2013). *Final Post Authorization Change Report and Revised Programmatic Environmental Impact Statement: Morganza to the Gulf of Mexico, Louisiana* (p. 122).

Van der Meer, J. W. (2002). Technical report wave run-up and wave overtopping at dikes. *TAW Report (Incorporated in the EurOtop Manual)*.

Zhang, J., Taflanidis, A. A., Nadal-Caraballo, N. C., Melby, J. A., & Diop, F. (2018). Advances in surrogate modeling for storm surge prediction: Storm selection and addressing characteristics related to climate change. *Natural Hazards*, *94*(3), 1225–1253.